ISCI, Volume *2*

Supplemental Information

An Early Function of Polycystin-2

for Left-Right Organizer Induction in *Xenopus*

Philipp Vick, Jennifer Kreis, Isabelle Schneider, Melanie Tingler, Maike Getwan, Thomas Thumberger, Tina Beyer, Axel Schweickert, and Martin Blum

Supplemental Figures and legends

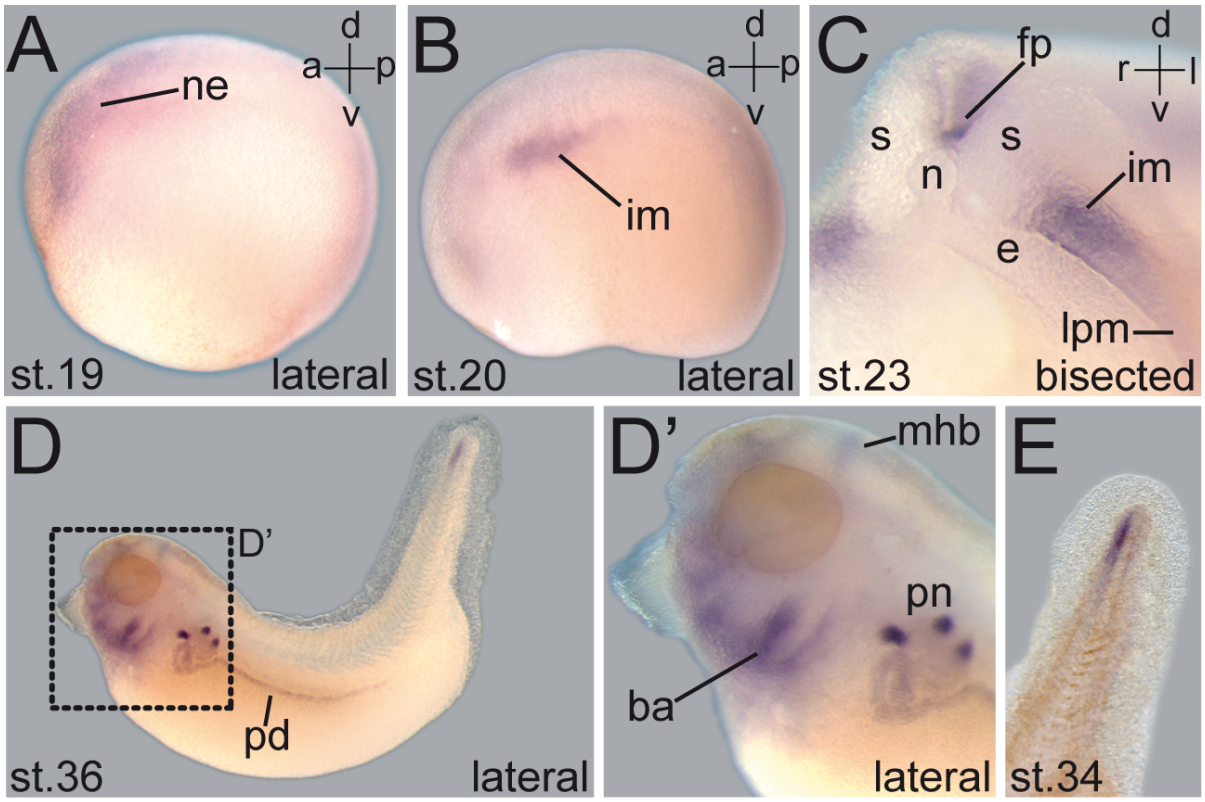

Figure S1: Related to Figure 1. Late expression pattern of *pkd2*.
Expression in the neuroectoderm (A-C), intermediate mesoderm (B, C), pronephric system (D), branchial arches (D') and tailbud (E) in early to late tailbud stages.
a, anterior; ba, branchial arches; d, dorsal; e, endoderm; fp, floorplate; im, intermediate mesoderm; l, left; lpm, lateral plate mesoderm; mhb, mid hindbrain boundary; n, notochord; ne, neuroectoderm; pd, pronephric duct; pn, pronephros; r, right; s, somites; v, ventral

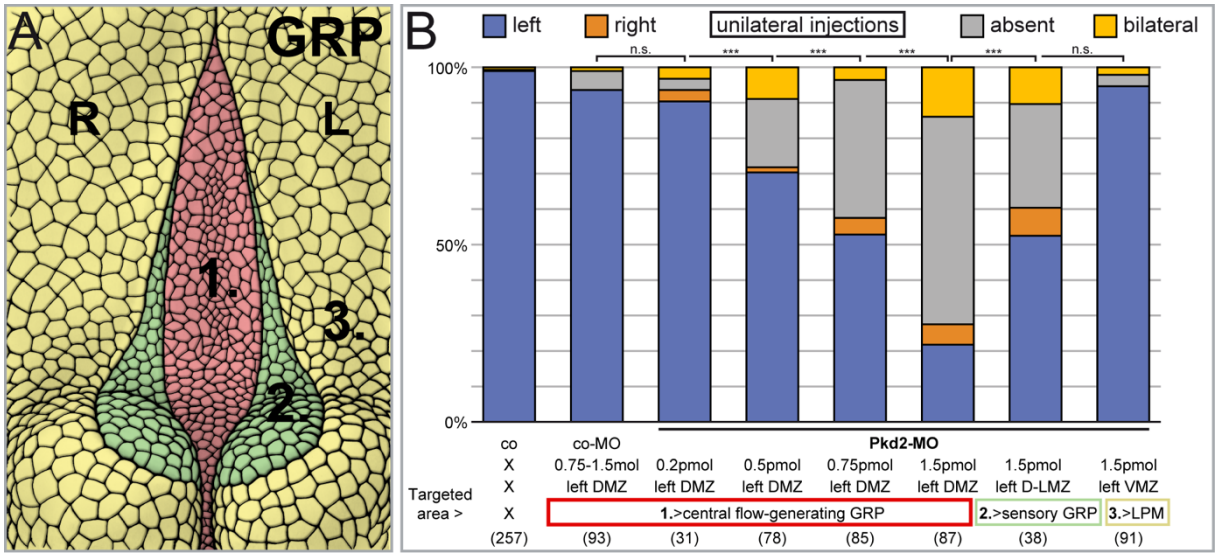

Figure S2: Related to Figure 2. Lineage-specific knockdown of *pkd2* reveals a left-sided dorsal requirement of Polycystin-2 in the LRO

(A) Schematic depiction of the differentially targeted areas of the gastrocoel roof in a dorsal explant of a stage 17 neurula embryo with the central, flow-generating population of the LRO (1. red), the lateral, sensory population of the LRO (2. green), and the surrounding endodermal cells (3. yellow) that cover the lateral plate mesoderm, which will express *nodal* and *pitx2c* on the left side after flow-dependent symmetry breakage to govern asymmetric organogenesis.

(B) Unilateral left-sided *pkd2* knockdown experiment showing dose-dependent loss of *pitx2c* when injected into the left dorsal marginal zone (DMZ) to target the central, flow-generating GRP. Injection into the dorso-lateral marginal zone (D-LMZ) to target the sensory part of the GRP (i.e. the lateral LRO cells) caused fewer, yet significant LR defects. Injecting the ventral marginal zone (VMZ) to target the left lateral plate mesoderm did not result in miss-expression of *pitx2c*.

*p<0.05, **p<0.01, **p<0.001 for all panels.

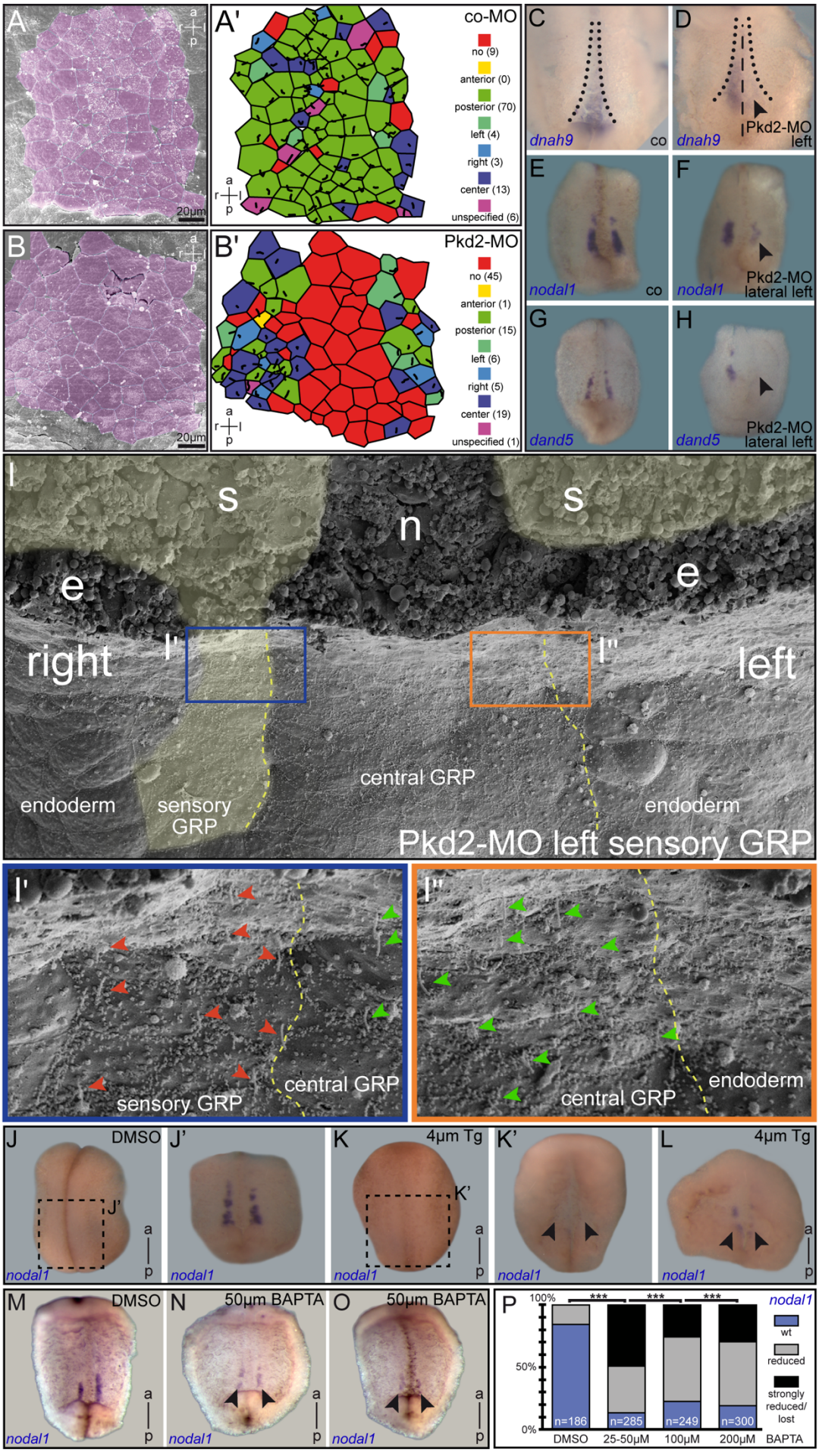
A
A'
co-MO
no (9)
anterior (0)
posterior (70)
left (4)
right (3)
center (13)
unspecified (6)
20µm
B
B'
Pkd2-MO
no (45)
anterior (1)
posterior (15)
left (6)
right (5)
center (19)
unspecified (1)
C
dnah9
co
D
dnah9
Pkd2-MO
left
E
nodal1
co
F
nodal1
Pkd2-MO
lateral left
G
dand5
H
dand5
Pkd2-MO
lateral left
I
s
n
s
e
e
right
I'
I"
left
central GRP
endoderm
sensory
GRP
endoderm
Pkd2-MO left sensory GRP
I'
sensory GRP
central GRP
I"
central GRP
endoderm
J
DMSO
J'
K
4µm Tg
K'
K'
L
4µm Tg
nodal1
M
DMSO
N
50µm BAPTA
O
50µm BAPTA
P
100%
50%
0%
***
***
***
nodal1
wt
reduced
strongly
reduced/
lost
n=186
n=285
n=249
n=300
DMSO
25-50µM
100µM
200µM
BAPTA

Figure S3: Related to Figure 3. GRP defects in *pkd2* morphants

(A, B) SEM analysis of co-MO (A) and Pkd2-MO (B) injected specimens reveal loss of ciliation and altered GRP cell morphology in morphants. Examples are representative for 6 specimens analyzed each. Scale bars represent 20 micrometers.

(C-H) Unilateral absence of *dnah9* (D), *nodal1* (F) and *dand5* (H) in left-injected embryos in comparison to internal control sides at stage 17. Control embryos (C, E, G) show wildtype expression levels.

(I) SEM analysis of ciliation and cell morphology in dorsal explant of stage 17 specimen unilaterally injected with Pkd2-MO targeted exclusively to the lateral, sensory part of the GRP. Shown is a ventral view of the GRP broken transversally and revealing the deep tissue arrangements in the top half of the picture. Right (I') and left (I'') magnifications show both the sensory areas of the GRP. Note that the lateral GRP cells were absent on the MO-injected side, such that central GRP cells, which are characterized by posteriorly polarized cilia, directly bordered non-ciliated endodermal cells. Sensory GRP cilia highlighted with red arrowheads, central GRP cilia with green arrowheads.

(J-L) Expression of *nodal1* in lateral GRP cells of flow stage (st. 17) specimens following Tp (K, L) or 1% DMSO (J) treatment during mid to late gastrula stage (st. 11.5). *nodal1* was lost (K') or strongly reduced (L) after Tp treatment, without causing gastrulation defects.

(M-P) Expression of *nodal1* in lateral GRP cells of flow stage (st. 16-19) specimens following 25-200µM BAPTA-AM (N-P) or 0.05-1% DMSO (M, P) treatment during mid and late gastrula stages (st. 11.5-13/14). *nodal1* was lost (O) or reduced (N) after BAPTA-AM treatment.

*p<0.05, **p<0.01, **p<0.001

Black arrowheads indicate reduction or lack of expression.

a, anterior; e, endoderm; l, left; n, notochord; p, posterior; r, right; s, somites

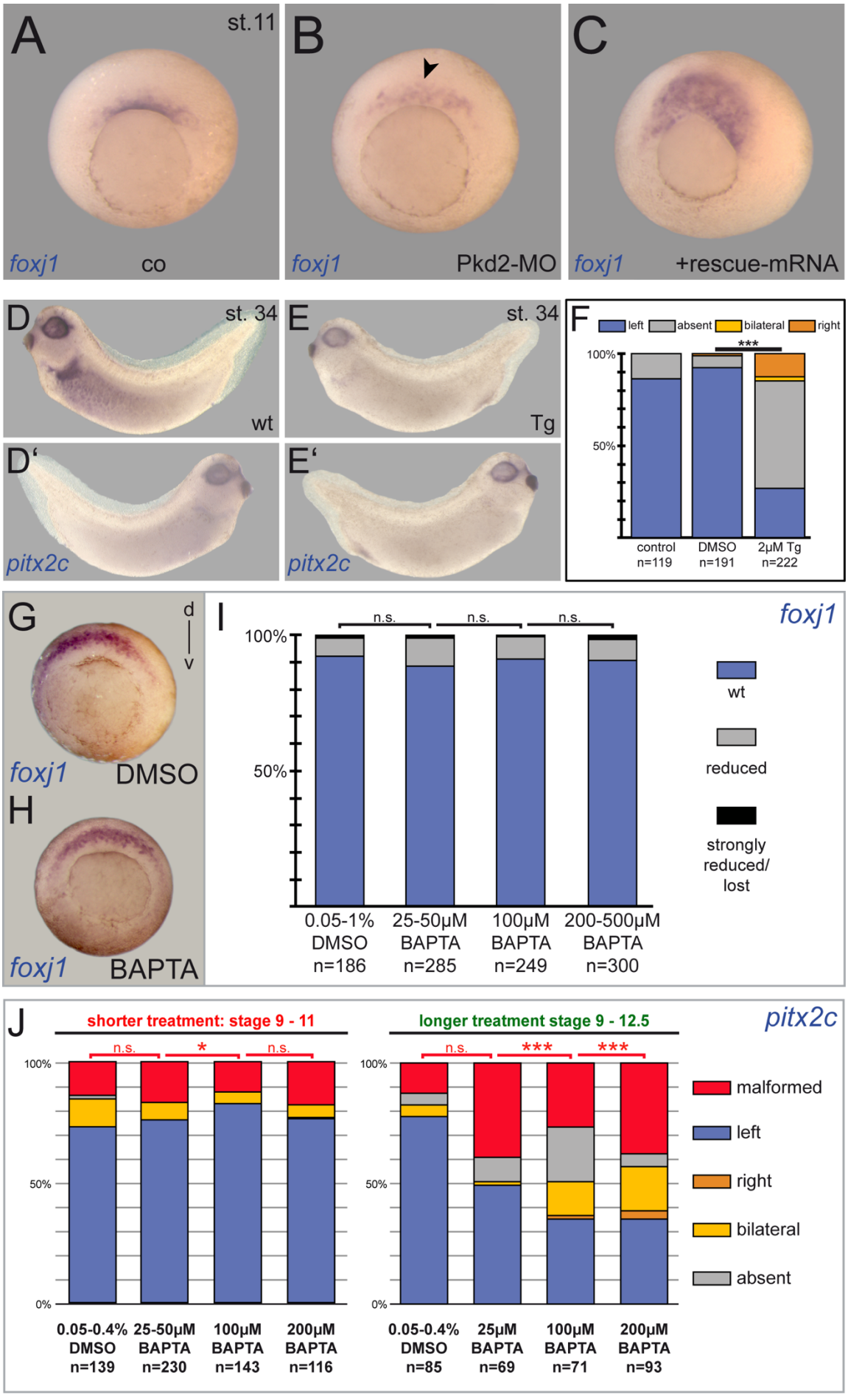
A
st.11
foxj1
co
B
foxj1
Pkd2-MO
C
foxj1
+rescue-mRNA
D
st. 34
wt
E
st. 34
Tg
D'
pitx2c
E'
pitx2c
F
left
absent
bilateral
right
***
100%
50%
control
n=119
DMSO
n=191
2µM Tg
n=222
G
d
v
foxj1
DMSO
H
foxj1
BAPTA
I
foxj1
n.s.
n.s.
n.s.
100%
50%
0.05-1%
DMSO
n=186
25-50µM
BAPTA
n=285
100µM
BAPTA
n=249
200-500µM
BAPTA
n=300
wt
reduced
strongly
reduced/
lost
J
pitx2c
shorter treatment: stage 9 - 11
longer treatment stage 9 - 12.5
n.s.
*
n.s.
n.s.
***
***
100%
50%
0%
0.05-0.4%
DMSO
n=139
25-50µM
BAPTA
n=230
100µM
BAPTA
n=143
200µM
BAPTA
n=116
0.05-0.4%
DMSO
n=85
25µM
BAPTA
n=69
100µM
BAPTA
n=71
200µM
BAPTA
n=93
malformed
left
right
bilateral
absent

Figure S4: Related to Figure 4. Calcium manipulating agents Thapsigargin or BAPTA-AM impacted differently on LR development

(A-C) *foxj1* expression (A) was reduced in *pkd2* morphants (B) and rescued upon co-injection of Pkd2-MO and a full-length *pkd2* rescue mRNA not targeted by the MO (C).

(D-F) A 20-minute thapsigargin treatment before gastrulation resulted in loss of *pitx2c* expression in >50% of embryos without concomitant gastrulation defects, reminiscent of Pkd2-MO injected specimens (cf. Figure 2D).

(G-J) Treatment of embryos between blastula (st. 9) and early gastrula stages (st. 10.5) with different concentrations of the calcium chelator BAPTA-AM did not reduce *foxj1* expression (H, I), in comparison to 0.05-1.00% DMSO treatment (G, I). (J) Embryos analyzed for *pitx2c* expression at tailbud stages after short (left side, until stage 11) or long (right side, until stage 12.5) treatment with BAPTA-AM. Longer (st. 9-12.5), but not short treatment (st. 9-11) resulted in significant LR defects. Please note the high proportion of embryos with general axis malformations when treated until late gastrulation (right side) as compared to shorter treatment (left side). Significances in (J) were calculated for LR expression patterns of *pitx2c* only, not including malformed embryos, which are also shown in the graph.

*p<0.05, **p<0.01, **p<0.001 for all panels.

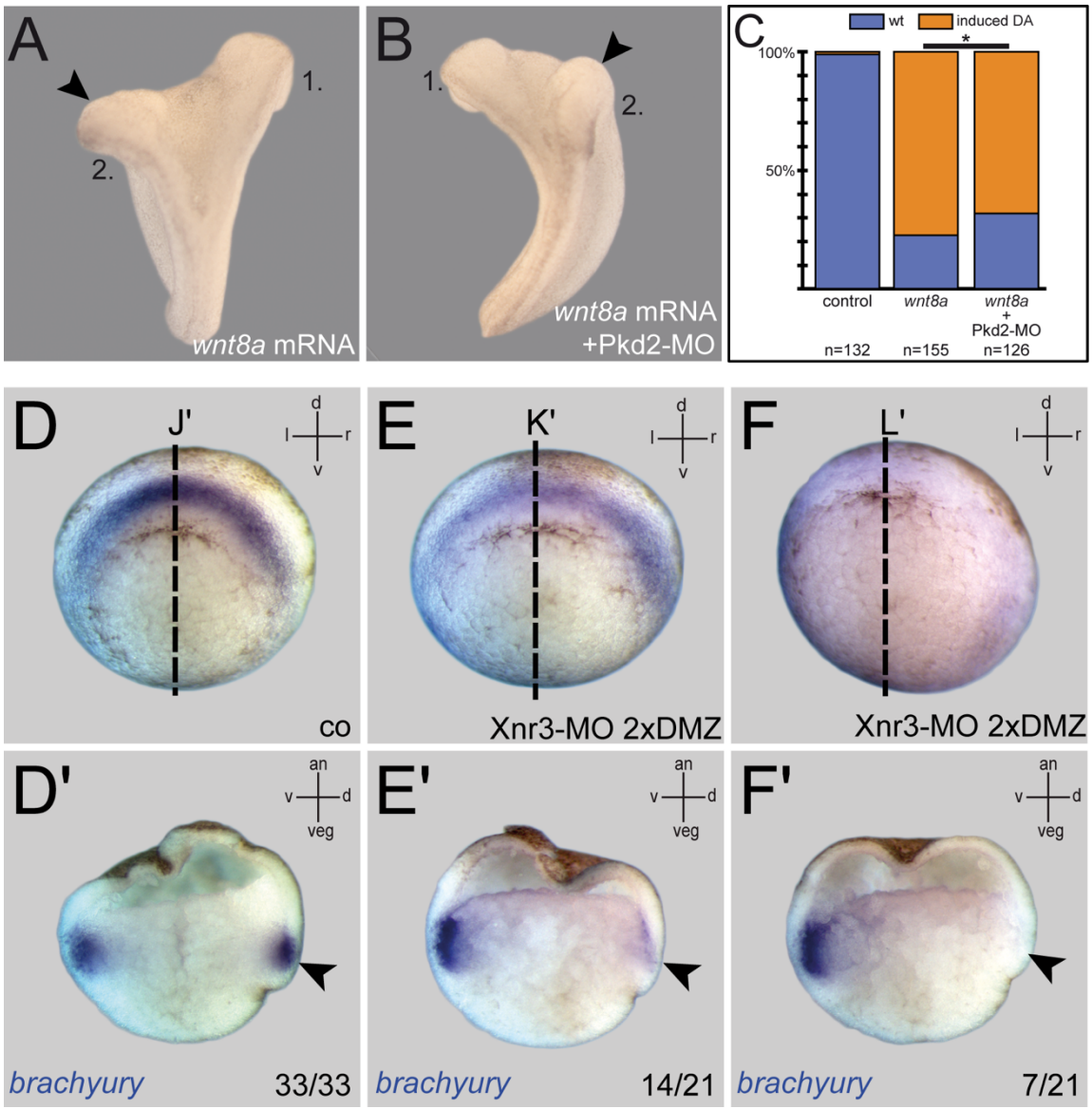

Figure S5: Related to Figure 4. Polycystin-2 function in LR axis formation is independent of canonical Wnt signaling

(A-C) Wnt-dependent double axis formation. Injection of *wnt8a* mRNA resulted in >75% of conjoined twinning (A, C). Co-injection of Pkd2-MO resulted in a very moderate drop of twinning rates to approx. 70% (B, C). Quantification of results (C). Arrowhead indicates induced secondary axis.

(D-F) Wildtype expression of *brachyury* during gastrulation in control specimens (D) was reduced (E) or lost (F) after injection of Xnr3-MO into the dorsal marginal zone (DMZ), demonstrating that Xnr3 was required for dorsal *bra* expression. Bisected embryos in D', E' and F' highlight these effects.

TRANSPARENT METHODS

CONTACT FOR REAGENT AND RESOURCE SHARING

Further information and requests for resources and reagents should be directed to and will be fulfilled by the Lead Contact, Philipp Vick (philipp.vick@uni-hohenheim.de).

EXPERIMENTAL MODEL AND SUBJECT DETAIL

For *in vivo* studies, *Xenopus laevis* was used as model organism. Frogs were obtained from Nasco (901 Janesville Avenue P.O. Box 901 Fort Atkinson). Handling, care and experimental manipulations of animals was approved by the Regional Government Stuttgart, Germany (Vorhaben A379/12 ZO „Molekulare Embryologie“), according to German regulations and laws (§6, article 1, sentence 2, nr. 4 of the animal protection act). Animals were kept at the appropriate condition (pH=7.7, 20°C) at a 12 h light cycle in the animal facility of the Institute of Zoology of the University of Hohenheim. Female frogs (4-20 years old) were stimulated with 25-75 units of human chorionic gonadotropin (hCG; Sigma), depending on weight and age, that was injected subcutaneously one week prior to oviposition. On the day prior to ovulation, female frogs were injected with 300-700 units of hCG (10-12 h before). Eggs were collected into a petri dish by carefully squeezing of the females and *in vitro* fertilized. Sperm of male frogs was gained by dissecting of the testes that was stored at 4°C in 1x MBSH (Modified Barth`s saline with HEPES) solution.

METHOD DETAILS

Plasmid construction

For *xnr3* mRNA-rescue experiments, the *xnr3* coding sequence was isolated from the original plasmid using Pfu DNA polymerase and sub-cloned into the CS2+ plasmid with EcoRI and XhoI restriction sites with the following oligonucleotides for PCR:

Xnr3.1 forward primer: 5’ CCGGAATTCATGGCATTTCTGAACCTG 3’
Xnr3.1 reverse primer: 5’ CCGCTCGAGTTACATGTCCTTGAATCC 3’

For *in vitro* synthesis of mRNA using the Ambion sp6 message kit, the plasmid was linearized with NotI.

Microinjections

Embryos were injected at the 4- to 8-cell stage, using a Harvard Apparatus. Drop size was calibrated to 4-6 nl / injection, amounts of injected MOs are indicated in the main text. Lineage tracers used for injection control were fluorescein (70,000 MW) or rhodamine B dextran (10,000 MW; both ThermoFisher). More detailed lineage-specific injections to target GRP and ventro-lateral tissues have been described previously (Blum et al., 2009a).

Treatments with calcium inhibitors

To manipulate intracellular calcium levels and wave patterns, embryos were incubated at two different time points, either with the ER SERCA-pump inhibitor Thapsigargin, or

with BAPTA-AM (cell-permeable form of the calcium-chelator BAPTA), both diluted in 0.1x MBSH.
For *foxj1* induction, embryos were incubated at stage 9 (before start of gastrulation) for 10, 15 or 20 min in 2µM Tg, then solution was replaced by 0.1x MBSH and embryos fixed at stage 10.5. Most robust effects were obtained with 15 or 20 min treatments, longer treatments with this concentration started to impact on gastrulation. Alternatively, ca. 120 min treatment with 0.75µM caused similar results (not shown). A similar procedure was applied for BAPTA-AM but solution was not replaced until fixation at stage 10.5 (begin of gastrulation). Tested concentration range was as indicated in Figure S4.
For analysis of *nodal1* induction, embryos were incubated in 4µM Tg, or in BAPTA-AM as indicated in Figure S3, both from stage 11.5 on to avoid gastrulation defects, and embryos were fixed at stage 15-18 (during flow-stages) for analysis by ISH.
For complementary *pitx2c* analyses, some embryos were reared until tailbud stages and processed for ISH after washout of the drug.

Immunofluorescence staining
For immunofluorescence staining, embryos were fixed in 4% PFA (Polyoxymethylene) for 1h at RT on a rocking platform, followed by 2 washes in 1x PBS^- for 15 min each. For staining of GRP explants, embryos were manually dissected transversally using a razor blade. Posterior halves (GRP explants) were collected and transferred to a 24 well plate and washed twice for 15 min in PBST. GRP-explants and whole embryos were blocked for 2h at RT in CAS-Block diluted 1:10 in PBST (0.1% Triton X-100). The blocking reagent was replaced by antibody solution (anti-acetylated tubulin antibody, 1:700 in CAS-Block) and incubated ON at 4°C. Antibody solution was removed and explants washed twice for 15 min in PBS, then the secondary antibody (1:1000 in CAS-Block) was added. Alexa Fluor 488 Phalloidin (1:200) was incubated over-night. Before photo documentation with a Zeiss LSM 700 Axioplan2 Imaging microscope, embryos or explants were shortly washed in PBS^- and transferred onto a microscope slide.

SEM and GRP Analysis
co-MO or Pkd2-MO injected specimens were fixed with 4% paraformaldehyde/ 2.5% glutaraldehyde and processed for SEM analysis. SEM photographs were analyzed for ciliation, polarization and cell surface area by individual full GRP analysis using ImageJ and evaluated as described (Beyer et al., 2012; Sbalzarini and Koumoutsakos, 2005).

Whole-mount in situ hybridization (ISH)
Embryos were fixed in MEMFA for 2h and processed following standard protocols (Sive et al., 2000). RNA *in situ* probes were transcribed using SP6 or T7 polymerases. In situ hybridization was modified from (Belo et al., 1997).

Flow-analysis
For analysis of leftward flow, dorsal posterior GRP-explants were dissected from stage 16/17 embryos injected with Pkd2-MO/co-MO and the lineage tracer rhodamine-B dextran (0.5 mg/ml) into one or two dorsal blastomeres. GRP-explants were placed in a petri-dish containing fluorescent microbeads (diameter 0.5 µm; diluted 1:2500 in

1xMBSH) and incubated for a few seconds. Explants were transferred to a microscope slide which was prepared with vacuum grease to create a small chamber that contained fluorescent microbeads solution; a cover slip carefully pressed on to seal the chamber. Time lapse movies of leftward flow were recorded using a AxioCam HSm video camera (Zeiss) at 2 frames per second using an Axioplan2 imaging microscope (Zeiss). For flow analysis, ImageJ and statistical-R, were used. Using the Particle-Tracker plug-in from ImageJ, leftward flow was analyzed and particle movement was measured, and data processed as described previously to create corresponding GTTs (Gradient Time Trails) as shown in Figure 3 (Vick et al., 2009).

Axis induction Assay

Double axis induction was performed by single injection of 40-80pg *wnt8a* mRNA with or without 1pmol Pkd2-MO into one ventral mesodermal blastomere at the 4-8 cell stage. Embryos were cultured until late tailbud stage and scored for double axis induction.

QUANTIFICATION AND STATISTICAL ANALYSIS

Statistical analysis

Statistical calculations of marker gene expression patterns and cilia distribution were performed using Pearson's chi-square test (Bonferroni corrected). For statistical calculation of ciliation, cilia length, cell size, flow velocity and directionality Wilcoxon-Match-Pair test was used (statistical R).

*=$p<0.05$, **=$p<0.01$, ***=$p<0.001$ were used for all statistical analyses.

KEY RESOURCES TABLE

REAGENT or RESOURCE	SOURCE	IDENTIFIER
Antibodies		
Mouse monoclonal anti acetylated α-tubulin	Sigma	AB_477585
Anti-mouse IgG (whole molecule) F(ab')2 fragment-Cy3	Sigma	AB_258785
Alexa Fluor 488 Phalloidin	Invitrogen	AB_2315147
Chemicals, Peptides, and Recombinant Proteins		
Pfu DNA Polymerase	Promega	M7745
FluoSpheres™ Carboxylate-Modified Microspheres, 0.5 µm, yellow-green fluorescent (505/515)	Invitrogen	F8813
Thapsigargin (3*S*,3a*R*,4*S*,6*S*,6a*R*,7*S*,8*S*,9b*S*)-6-(Acetyloxy)-4-(butyryloxy)-3,3a-dihydroxy-3,6,9-trimethyl-8-{[(2*Z*)-2-methylbut-2-enoyl]oxy}-2-oxo-2,3,3a,4,5,6,6a,7,8,9b-decahydroazuleno[4,5-*b*]furan-7-yl octanoate	Tocris	1138
BAPTA-AM 1,2-Bis(2-aminophenoxy)ethane-*N*,*N*,*N*',*N*'-tetraacetic acid tetrakis(acetoxymethyl ester)	abcam	Ab120503
Human chorionic gonadotropin (hCG)	Sigma	C0809-1VL
Critical Commercial Assays		
mMessage mMachine™ SP6 Transcription Kit	Thermo Fisher Scientific	AM1340
Experimental Models: Organisms/Strains		
Xenopus laevis (female, male)	Nasco	https://www.enasco.com/xenopus/
Oligonucleotides		
Xnr3.1 forward primer [5' CCGGAATTCATGGCATTTCTGAACCTG 3']	Sigma	
Xnr3.1 reverse primer [5' CCGCTCGAGTTACATGTCCTTGAATCC 3']	Sigma	
Software and Algorithms		
Adobe Suite CS6: Photoshop and Illustrator	Adobe	
ImageJ/Fiji		https://fiji.sc/
AxioVision 4.6	Zeiss	
Zen 2012 Blue edition	Zeiss	https://www.zeiss.com
Statistical R-Gui		https://www.r-project.org/
Other		
Pkd2-MO: 5' GGTTTGATTCTGCTGGGATTCATCG 3'	Gene Tools, Philomath, USA	(Tran et al., 2010)
Xnr3-MO: 5' TCTCTGGGTAGATTTGTGGTGACTC 3'	Gene Tools, Philomath, USA	
Nodal1-MO: 5' GCTGTCAGAAATGCCATGCTTGCAC 3'	Gene Tools, Philomath, USA	(Vonica and Brivanlou, 2007)
Dand5-MO1: 5' CTGGTGGCCTGGAACAACAGCATGT 3'	Gene Tools, Philomath, USA	(Vonica and Brivanlou, 2007)
Dand5-MO2: 5' TGGTGGCCTGGAACAACAGCATGTC 3'	Gene Tools, Philomath, USA	(Vonica and Brivanlou, 2007)
standard control-MO	Gene Tools, Philomath, USA	
Axioplan2 imaging microscope	Zeiss	
Zeiss LSM 700	Zeiss	
AxioCam HSm video camera	Zeiss	
Xenbase		https://xenbase.org
PubMed		https://www.ncbi.nlm.nih.gov/pubmed/

Supplemental References

Belo, J.A., Bouwmeester, T., Leyns, L., Kertesz, N., Gallo, M., Follettie, M., De Robertis, E.M., 1997. Cerberus-like is a secreted factor with neutralizing activity expressed in the anterior primitive endoderm of the mouse gastrula. Mechanisms of Development 68, 45–57.

Beyer, T., Danilchik, M., Thumberger, T., Vick, P., Tisler, M., Schneider, I., Bogusch, S., Andre, P., Ulmer, B., Walentek, P., Niesler, B., Blum, M., Schweickert, A., 2012. Serotonin Signaling Is Required for Wnt-Dependent GRP Specification and Leftward Flow in Xenopus. Current Biology 22, 33–39. doi:10.1016/j.cub.2011.11.027

Blum, M., Beyer, T., Weber, T., Vick, P., Andre, P., Bitzer, E., Schweickert, A., 2009. Xenopus, an ideal model system to study vertebrate left-right asymmetry. Dev. Dyn. 238, 1215–1225. doi:10.1002/dvdy.21855

Sbalzarini, I.F., Koumoutsakos, P., 2005. Feature point tracking and trajectory analysis for video imaging in cell biology. J. Struct. Biol. 151, 182–195. doi:10.1016/j.jsb.2005.06.002

Sive, H.L., Grainger, R.M., Harland, R.M., 2000. Early Development of Xenopus Laevis. CSHL Press.

Tran, U., Zakin, L., Schweickert, A., Agrawal, R., Doger, R., Blum, M., De Robertis, E.M., Wessely, O., 2010. The RNA-binding protein bicaudal C regulates polycystin 2 in the kidney by antagonizing miR-17 activity 137, 1107–1116. doi:10.1242/dev.046045

Vick, P., Schweickert, A., Weber, T., Eberhardt, M., Mencl, S., Shcherbakov, D., Beyer, T., Blum, M., 2009. Flow on the right side of the gastrocoel roof plate is dispensable for symmetry breakage in the frog Xenopus laevis. Developmental Biology 331, 281–291. doi:10.1016/j.ydbio.2009.05.547

Vonica, A., Brivanlou, A.H., 2007. The left–right axis is regulated by the interplay of Coco, Xnr1 and derrière in Xenopus embryos. Developmental Biology 303, 281–294. doi:10.1016/j.ydbio.2006.09.039